

# Effects of alamandine on monocrotaline-induced pulmonary hypertension in rats

Ava Soltani Hekmat<sup>1</sup>, Freshteh Amini<sup>1</sup>, Kazem Javanmardi<sup>1\*</sup>

<sup>1</sup> Department of Physiology, Fasa University of Medical Sciences, Fasa, Iran

## ARTICLE INFO

### Article type:

Original

### Article history:

Received: Sep 9, 2023

Accepted: Nov 11, 2023

### Keywords:

Alamandine  
Hypertension  
Monocrotaline  
Oxidative stress  
Pulmonary  
Renin-angiotensin system

## ABSTRACT

**Objective(s):** Pulmonary arterial hypertension (PAH) is a severe and often fatal disease that is associated with oxidative stress and inflammation. Alamandine, a component of the renin-angiotensin system, known for its antioxidative, anti-inflammatory, and antifibrotic effects, has been investigated in this study to determine if it has protective effects against PAH induced by monocrotaline (MCT) and if these effects are associated with oxidative stress, inflammatory factors, and inducible nitric oxide synthase (iNOS).

**Materials and Methods:** Rats were administered MCT (40 mg/kg) on day 0 and then received alamandine (50 mg/kg/day) via mini-osmotic pumps for 21 days starting one day later. Hemodynamic parameters, electrocardiograms, superoxide dismutase (SOD), catalase (CAT), malondialdehyde (MDA), inflammatory cytokines (TNF- $\alpha$ , IL-1 $\beta$ , and NF- $\kappa$ B), iNOS, and MrgD receptor expression in lung tissue were evaluated at the end of the 21-day period. The MrgD receptor was quantified through immunofluorescent staining, and the histopathology of lung tissues was evaluated using hematoxylin and eosin staining.

**Results:** The results showed that alamandine treatment significantly improved hemodynamic parameters, oxidative stress markers, inflammatory factors, and electrocardiographic data. Furthermore, treatment with alamandine decreased the levels of iNOS. Additionally, alamandine treatment decreased the expression levels of MrgD receptors in the lung tissue of MCT-induced PAH.

**Conclusion:** In summary, this study indicates that alamandine has protective effects against monocrotaline-induced PAH, and these effects may be attributed to the inhibition of oxidative stress, inflammatory parameters, and iNOS.

► Please cite this article as:

Soltani Hekmat A, Amini F, Javanmardi K. Effects of alamandine on monocrotaline-induced pulmonary hypertension in rats. Iran J Basic Med Sci 2024; 27: 500-508. doi: <https://dx.doi.org/10.22038/IJBMS.2023.74865.16254>

## Introduction

Pulmonary arterial hypertension (PAH) is characterized by elevated blood pressure in the pulmonary arteries, leading to increased mortality risks. The contemporary definition of PAH has been reshaped by recent outcome data, placing emphasis on early detection. According to the updated criteria, PAH is diagnosed in individuals with a mean pulmonary artery pressure exceeding 20 mmHg, as confirmed by right heart catheterization (1). The growing prevalence of PAH is influenced by an aging population, increased incidence of heart and lung diseases, and improved survival rates due to targeted therapies (2).

A hallmark of PAH is the proliferation of vascular wall cells and the remodeling of precapillary arteries, causing elevated pulmonary artery pressure and eventual right ventricular failure (3, 4). This condition is underlined by various degrees of pulmonary arterial vessel remodeling, resulting in increased mean pulmonary artery pressure, pulmonary vascular resistance, and subsequently, right ventricular hypertrophy (RVH) and failure (4, 5).

The pathology of PAH is multifaceted, rooted in endothelial dysfunction, which manifests as an imbalance between vasoconstrictive and vasodilatory factors such as endothelin and nitric oxide (NO). This imbalance instigates pulmonary vasoconstriction and vascular remodeling, leading to a persistent rise in pulmonary vascular resistance (6). Furthermore, cytokines play a pivotal role in PAH's

pathogenesis (7).

Inflammation stands out as a fundamental hallmark in the pathophysiology of PAH. Clinical and foundational research consistently underlines its significance in PAH development (8). One of the manifestations of this is seen in the fact that PAH is frequently a complication of autoimmune diseases, including systemic sclerosis, HIV infection, and schistosomiasis. Moreover, perivascular inflammation is commonly seen in various PAH types, as evidenced by cellular markers such as the infiltration of mast cells, T and B lymphocytes, and macrophages around the vessels (9). Another telltale sign is the elevated levels of cytokines like tumor necrosis factor (TNF), interleukin-1 (IL-1), and interleukin-6 (IL-6) in both lung tissue and blood (10). These cytokines are more than just markers; they potentially serve diagnostic and prognostic purposes in PAH. For instance, elevated serum IL-1 $\beta$  levels in PAH patients have been directly linked with unfavorable outcomes (8, 11).

On a parallel front, oxidative stress has emerged as a pivotal factor in PAH's development, with multiple studies supporting this connection (12). Central to this are the disturbances observed in the reactive oxygen species and NO signaling pathways. An upset in the oxidant/antioxidant equilibrium adversely affects vascular tone, precipitating the abnormal activation of antiapoptotic and mitogenic routes. This, in turn, drives unchecked cell growth and

\*Corresponding author: Kazem Javanmardi. Department of Physiology Fasa University of Medical Sciences Ebn-E-Sina SQ, Fasa, Iran. Email: [kjavanmardi@fums.ac.ir](mailto:kjavanmardi@fums.ac.ir)

culminates in vasculature obliteration (13). In experimental setups, interventions using antioxidants have demonstrated potential protective effects against PAH (13).

While the introduction of advanced pharmaceuticals like prostanoids, endothelin receptor antagonists, and phosphodiesterase-5 inhibitors has revolutionized PAH prognosis, the challenge remains. The persistently high morbidity and mortality rates underscore an unmet need (14). There is an imperative demand for innovative PAH therapeutic strategies that are intricately woven with its detailed pathophysiology.

One such potential avenue is the renin-angiotensin system (RAS). All major RAS components are expressed in lung tissues, making it pivotal for lung pathophysiology (15). Alamandine is a new member of the angiotensin family that has exhibited significant cardioprotective effects in rats treated with isoproterenol. This peptide is similar to Ang-(1-7) and can bind to the Mas-related G-coupled receptor known as member D (MrgD) (15, 16). Alamandine has both antifibrotic and anti-inflammatory effects (17, 18). It increases antioxidant expression in ventricles exposed to ischemia-reperfusion injury (19) and reduces pro-inflammatory factors induced by aortic constriction, such as TNF- $\alpha$  and IL-1 $\alpha$ , in mice (20). In a study on an animal model of sepsis induction by polysaccharides in C57BL/6J mice, the plasma and tissue levels of IL-1 $\beta$  and TNF $\alpha$  increased. Administration of alamandine reduced the levels of inflammatory cytokines and apoptosis in cardiac tissues (21).

Based on the antioxidant and anti-inflammatory effects of alamandine, we hypothesize that the activation of the protective arm of the RAS by alamandine may attenuate various characteristics of PAH in a rat pulmonary hypertension model through biochemical, hemodynamic, and histopathological studies.

## Materials and Methods

Male Sprague-Dawley rats, aged 6–8 weeks (weight = 200–220 g), were housed in groups of five in a temperature-controlled room maintained at 22 $\pm$ 2 °C with a 12:12-hr light-dark cycle, lights on at 7:00 AM. The animals were provided free access to standard laboratory chow and water. All experimental protocols conformed to the National Institutes of Health Guide for the Care and Use of Laboratory Animals and were approved by Fasa University of Medical Sciences, Iran, with the ethical code (IR.FUMS.AEC.1401.010), obtained on September 7, 2022. A total of 28 rats were used in this study, divided into 4 groups of 7 rats each.

For biochemical and hemodynamic studies, rats were anesthetized via intraperitoneal ketamine (70 mg/kg) and xylazine (30 mg/kg). The anesthesia level was evaluated using the toe-pinch reflex.

### Experimental protocols

In this study, we used monocrotaline (MCT) for induction of pulmonary hypertension. The advantages of the MCT model are its technical simplicity, reproducibility, and relatively low cost (5). Subjects were randomly allocated into various experimental and control groups. To ensure impartiality and accuracy in results, all stages of the study, including selection, treatment, and outcome assessment, were conducted in a blinded manner. Rats were divided randomly into the following groups:

**Control Group (Group I):** In the control group, saline

was administered via mini-osmotic pumps (model 2006; ALZET Osmotic Pumps, CA, USA) at an infusion rate of 0.15  $\mu$ l/hr, mirroring the administration method employed for the experimental groups. Additionally, rats in this group received an intraperitoneal (IP) injection of saline to maintain consistency with the injection protocol used in the other groups.

**MCT Group (Group II):** Rats in this group received an IP injection of 40 mg/kg MCT (22) on day 0. Due to the restrictions imposed by the local animal ethics and welfare committee rules, experiments involving rats exposed to 40 mg/kg MCT were limited to 25 days. Therefore, right ventricular pressure and other parameters were measured on day 22 after MCT injection, as this was the final day of the experimental period to avoid the risk of end-stage heart failure and premature death observed in previous experiments (22).

**Ala Group (Group III):** Rats in this group were administered alamandine (Phoenix Pharmaceuticals Inc., CA, USA) for 21 days via mini-osmotic pumps with an infusion rate of 0.15  $\mu$ l/hr (approximately 50  $\mu$ g alamandine/kg/day) (23–26) starting from day 1.

**MCT+Ala Group (Group IV):** In this group, rats received alamandine via mini-osmotic pumps for 21 days (approximately 50  $\mu$ g alamandine/kg/day), starting from day 1, and an IP injection of MCT in normal saline (40 mg/kg) on day 0.

### Measurements of right ventricular systolic pressure and weight

Rats were anesthetized with ketamine (Yuhan, Korea) and xylazine to measure right ventricular systolic pressure (RVSP) 22 days after MCT injection (Bayer Korea, Korea). The pressure transducer was inserted into the RV through the right jugular vein and connected to PowerLab (AD Instruments Pty. Ltd, Australia). Following stabilization, RVSP was measured for 10 min and blood was drawn from the abdominal aorta (27). Hearts and lungs were promptly removed and weighed. The right lungs were dissected and perfused with ice-cold phosphate-buffered saline, then snap-frozen in liquid nitrogen and stored at -80 °C for subsequent biochemical analyses. The left lung was embedded in 10% formalin for histopathological and immunofluorescent staining.

### Electrocardiogram

Electrocardiogram (ECG) traces were recorded on day 22 before the rats were sacrificed. Needle electrodes were placed under the skin of the animals in the lead II position. ECG parameters were recorded with PowerLabs and LabChart software (AD Instruments, Australia).

### Measurements of cytokine concentrations in lung tissue

Cytokine levels (IL-1 $\beta$ , TNF- $\alpha$ , IL-6, and NF- $\kappa$ B) were assessed using ELISA kits from ZellBio GmbH (Germany). The quantitative ELISA sandwich technique was employed for quantification in lung tissues. In this method, 100  $\mu$ l of standard or sample solutions were added to microplate wells and incubated at 37 °C for 2 hr. Biotin-conjugated antibodies specific to the targeted cytokines were added to each well for an additional hour at 37 °C. After washing, avidin conjugated with horseradish peroxidase was added, followed by incubation at 37 °C for 1 hr. A chromogenic substrate solution produced a color proportionate to

cytokine concentration. The enzyme-substrate reaction was stopped with a stop solution. Color changes were measured by recording optical density (OD) at 450 nm using a Bio Tek ELISA reader. Cytokine concentrations were determined by comparing sample OD values to a standard curve generated with known standard concentrations (28).

#### **Measurements of lung tissue oxidants and anti-oxidative enzymes**

The left lung was resected after being washed with saline via the pulmonary artery. A nine-fold volume of phosphate-buffered saline (PBS) was added before gentle grinding at 4 °C. The levels of SOD, CAT, and MDA in lung tissue homogenates were measured using a colorimetric technique and matching kits.

#### **Measurement of MDA**

The MDA measurements were conducted using a thiobarbituric acid reaction method with the MDA assay kit (Cat No: ZB-MDA) from ZellBio GmbH (Germany). For the analysis, 0.15 ml of the sample was placed in a designated sample tube, 0.15 ml of a standard solution in the standard tube, and 0.15 ml of dehydrated alcohol in the blank testing tube. Then, 4 ml of a mixed reagent was added to each tube. After thorough mixing and incubation at 95 °C for 40 min, the specimens were cooled in running water and centrifuged at 3500 rpm for 10 min. Finally, the supernatant from each tube underwent colorimetric analysis at 532 nm (with zero adjustment using distilled water) (29).

#### **Measurement of SOD**

SOD activity was determined using the SOD assay kit (Cat No: ZB-SOD) from ZellBio GmbH (Germany) with the WST-1 method. Control wells contained a mixture of double distilled water, enzyme working solution, and substrate application solution. Blank control wells had a mixture of double distilled water, enzyme dilution solution, and substrate application solution. Measurement wells were prepared by combining these mixtures. After incubation at 37 °C, absorbance at 450 nm was measured using a microplate reader (29).

#### **Measurement of CAT**

In the CAT assay using the ZellBio ELISA kit, assay buffer was added to the wells. A mixture of methanol and the sample was introduced. Diluted hydrogen peroxide was added to initiate enzymatic reactions. The plate was incubated for 20 min at room temperature. The reaction was terminated with potassium hydroxide and catalase periodate. After further incubation, catalase potassium periodate was added. Absorbance was measured at 540 nm (29).

#### **Measurement of iNOS**

NO levels in lung tissue were measured using an ELISA kit (MyBioSource, Cat No: MBS263618). This competitive enzyme immunoassay method used an anti-iNOS monoclonal antibody and iNOS-HRP conjugate. Lung samples and buffer were incubated with the iNOS-HRP conjugate on a pre-coated plate for one hour. After incubation, wells were washed, and an HRP enzyme substrate was added, resulting in a blue complex. The reaction was stopped with a stop solution, turning the solution yellow, and the yellow color intensity was measured at 450 nm using a microplate reader (30).

#### **Histopathological studies**

We randomly selected three left lung tissue specimens from each group. These specimens were fixed in 10% neutral buffered formalin for 48 hr, followed by an additional 48-hour immersion in 10% neutral buffered formalin for optimal preservation. The specimens underwent systematic dehydration in graded alcohol concentrations, residual alcohol was removed with xylene treatment, and they were expertly embedded in paraffin. The resulting paraffin blocks were sectioned into 5- $\mu$ m-thick slices using a microtome, floated on a water bath, mounted on microscope slides, and dried in a 60 °C oven for 20 min. Sections were meticulously stained with hematoxylin and eosin to highlight histopathological features. A blind evaluation was performed on three randomly selected sections from each animal, resulting in a total of 15 images per animal. Numerical results were recorded for histopathological tests to ensure transparency and replicable analysis. Images at 40x magnification were analyzed at five random points within each section using Image J software. This rigorous methodology ensured the accuracy and impartiality of our histopathological assessments.

#### **MrgD receptor measurement by immunofluorescent staining**

Paraffin-embedded lung tissue sections (5  $\mu$ m thick) underwent immunofluorescence analysis. The process included deparaffinization, rehydration, and PBS washing. To enhance cell membrane permeability, Triton was applied. Unwanted secondary antibody reactions were prevented by incubating samples in goat serum. Primary antibodies were applied, followed by refrigeration for 24 hr. After primary antibody incubation, samples were washed and secondary antibodies were added, followed by incubation. The samples were washed again and treated with DAPI. Glycerol and PBS were applied for visualization, and samples were examined using fluorescent microscopy. Marker intensity was quantified as a percentage of green color in the image. This rigorous immunofluorescence protocol ensured precise marker assessment in the lung tissue sections.

#### **Statistical analysis**

The statistical analysis was conducted using two-way analysis of variance (ANOVA), followed by *post hoc* Tukey test to examine the differences between the means of groups. This analysis was performed using SPSS version 27. For generating the figures, GraphPad Prism 7.04 (GraphPad Software, USA) was utilized. The statistical significance threshold was set at  $P < 0.05$ .

## **Results**

### **Hemodynamics**

In our rat model of PAH, MCT injection led to significant hemodynamic changes. RVSP increased to  $47.78 \pm 1.90$  mmHg in the MCT group compared to the control group's  $20.97 \pm 1.70$  mmHg ( $P < 0.001$ ), mitigated by Alamandine co-treatment (MCT+Ala group:  $29.26 \pm 2.30$  mmHg,  $P < 0.001$ ).

RV hypertrophy, indicated by the RV/(LV+SP) weight ratio, increased in the MCT group to  $0.41 \pm 0.04$  ( $P < 0.001$ ), significantly higher than the control group's  $0.22 \pm 0.02$ . The MCT+Ala group showed a moderate ratio of  $0.33 \pm 0.03$  ( $P < 0.001$ ).

Body weight in the MCT group decreased significantly to  $218.00 \pm 12.30$  g, compared to the control group's  $326.00 \pm 14.57$  g ( $P < 0.001$ ). Alamandine co-administration mitigated this loss, with the MCT+Ala group at  $260.00 \pm 21.13$  g.

**Table 1.** Comparison of right ventricular systolic pressure (RVSP), right ventricle to (left ventricle + septum) ratio (RV/(LV+SP) ratio), right ventricular weight to body weight ratio (RVW/BW), lung weight to body weight ratio (lung W/BW ratio), and body weight (BW) in monocrotaline-induced pulmonary hypertensive rats treated with alamandine, compared to the control group

	Control	Ala	MCT	MCT+Ala
RVSP (mmHg)	20.97±1.7	22.19±1.2	47.78±1.9***	29.26±2.3****
BW (g)	326±14.57	346± 15.9	218.0±12.3***	260.±21.13***
RVW/(LV+SP) ratio	0.22±0.02	0.21±0.01	0.41±0.04***	0.33±0.03****
RVW/BW (g/kg)	0.53±0.04	0.58±0.07	1.22±0.09***	0.87±0.03***
Lung W/BW ratio (mg/g)	3.69±0.1	3.53±0.6	6.18±0.2**	4.82±0.1**

The data are presented as mean ± standard deviation (SD); n=7 for each treatment group.

\* $P<0.05$ , \*\* $P<0.01$ , \*\*\* $P<0.001$  indicate statistical significance compared to the control group

# $P<0.05$ , ## $P<0.01$ , ### $P<0.001$  indicate statistical significance compared to the monocrotaline (MCT) group

The RVW/BW ratio in the MCT group was substantially higher at  $1.22 \pm 0.09$  g/kg compared to the control group's  $0.53 \pm 0.04$  g/kg ( $P<0.001$ ), moderated in the MCT+Ala group ( $0.87 \pm 0.03$  g/kg).

The lung W/BW ratio in the MCT group significantly increased to  $6.18 \pm 0.20$  compared to the control's  $3.69 \pm 0.10$  ( $P<0.01$ ), with alamandine co-treatment mitigating this rise in the MCT+Ala group ( $4.82 \pm 2.30$ ,  $P<0.001$ , Table 1).

### Electrocardiogram

MCT administration led to various electrocardiographic changes, including a significant decrease in heart rate, with the MCT group averaging  $248.30 \pm 60.70$  beats/minute, contrasting the control group's  $373.80 \pm 53.70$  beats/minute ( $P<0.05$ ). Alamandine co-treatment moderated this decline, resulting in a mean rate of  $332.60 \pm 98.90$  beats/minute in the MCT+Ala group, though this change wasn't statistically significant.

The P-R interval in the control group averaged  $48.80 \pm 5.80$  ms, while MCT treatment reduced it to  $45.40 \pm 11.80$  ms. Co-treatment with alamandine somewhat restored this, resulting in an average of  $47.30 \pm 10.30$  ms for the MCT+Ala group, with no statistically significant variances ( $P>0.05$ ).

MCT significantly reduced the QRS amplitude, with the control group at  $1.09 \pm 0.14$  mv and the MCT group at  $0.63 \pm 0.17$  mv ( $P<0.001$ ). Alamandine co-treatment moderated this effect, with the MCT+Ala group exhibiting an amplitude of  $1.04 \pm 0.16$  mv, a significant rebound from the MCT-only group ( $P<0.001$ ). Additional details and visual representation can be found in Table 2 and Figure 1.

### Effect of co-administration of alamandine and MCT on oxidative stress markers (MDA, SOD, and catalase) in lung tissue

MCT administration significantly increased lung MDA levels ( $16.82 \pm 4.92$   $\mu$ M) compared to the control group (2.88

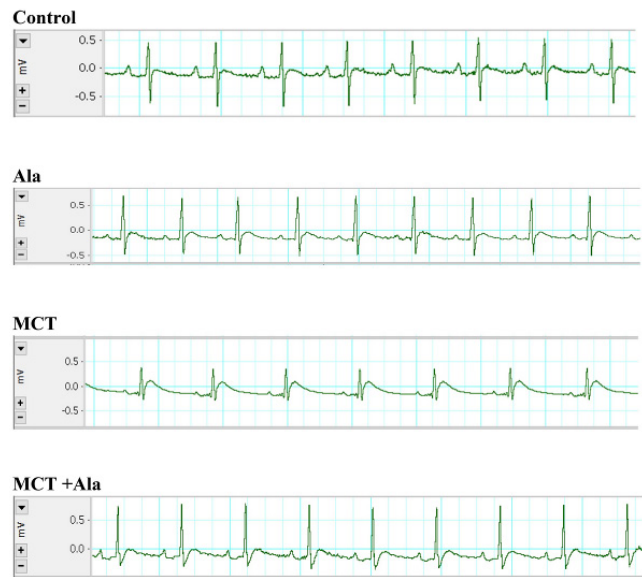


**Figure 1.** Electrocardiogram recordings from anesthetized rats across different experimental groups, comprising the control group, monocrotaline (MCT)-treated group, alamandine group, and MCT + alamandine group. Notably, the MCT-treated group exhibited significant reductions in heart rate, and QRS amplitude, which were effectively mitigated by alamandine. Ala: Alamandine; MCT: Monocrotaline

$\pm 1.79$   $\mu$ M,  $P<0.001$ ), while co-treatment with alamandine reduced MDA levels ( $0.96 \pm 0.23$   $\mu$ M) ( $P>0.05$ ).

MCT administration led to a notable reduction in SOD levels ( $13.03 \pm 5.93$  IU/ml) compared to the control group ( $36.32 \pm 12.11$  IU/ml,  $P<0.001$ ). Co-treatment with alamandine increased SOD levels ( $85.33 \pm 12.81$  IU/ml) ( $P<0.001$ ).

Catalase levels significantly decreased in lung tissue with MCT administration ( $44.88 \pm 8.74$   $\mu$ M/ml) compared to

**Table 2.** Assessment of electrocardiographic parameters in various experimental groups: Comparative analysis of heart rate, P-R interval, and QRS amplitude in control, alamandine-administered, monocrotaline (MCT)-treated, and MCT + alamandine-treated rats

Title 1	Control	Ala	MCT	MCT+Ala
HR (bpm)	373.8±53.7	361.1±58.2	248.3±60.7*	332.6±98.9
P-R interval (ms)	48.8±5.8	49.2±6.8	45.4±11.8	47.3±10.3
QRS amplitude (mv)	1.08±0.14	1.11±0.15	0.63±0.17***	1.04±0.16##

Data are expressed as mean ± SD; n = 7 for each group

Ala: Alamandine; MCT: Monocrotaline; HR:Heart rate; bpm: Beat per minute; ECG: Electrocardiogram

\* $P<0.05$ , \*\*\* $P<0.001$  compared to the control; ## $P<0.001$  compared to the MCT group.

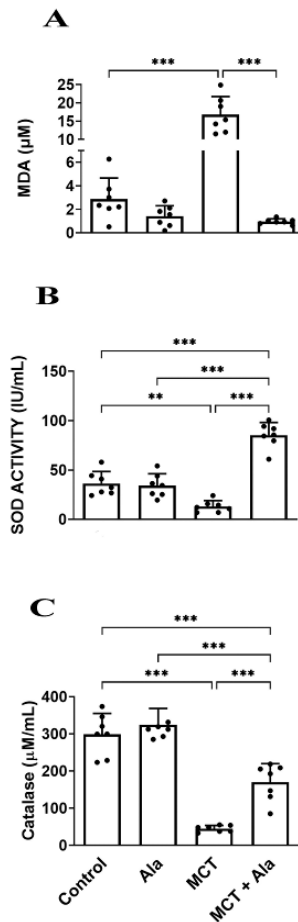


**Figure 2.** Oxidative stress markers in rats with monocrotaline (MCT)-induced pulmonary hypertension

(A) Malondialdehyde (MDA) levels in lung tissue, (B) Superoxide dismutase (SOD) activity in lung tissue, and (C) Catalase activity in lung tissue (data presented as mean  $\pm$  SD, n=7). Statistical comparisons were performed using a two-way analysis of variance (ANOVA) followed by Tukey's post hoc test.

The significance levels are represented as \* $P$ <0.05, \*\* $P$ <0.01, and \*\*\* $P$ <0.001.

the control group ( $298.70 \pm 56.11 \mu\text{M/ml}$ ,  $P$ <0.001). Co-treatment with alamandine partially reversed this effect ( $169.90 \pm 49.73 \mu\text{M/ml}$ ) ( $P$ >0.05) (Figure 2).

#### Effect of co-administration of alamandine and MCT on iNOS in lung tissue

MCT administration significantly increased iNOS levels to  $345.10 \pm 29.78 \text{ ng/ml}$  compared to the control group's

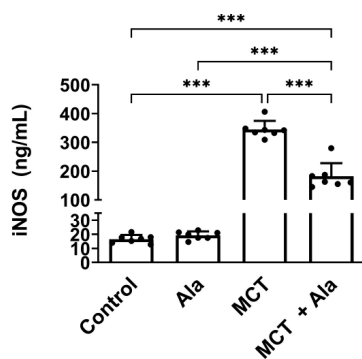


**Figure 3.** Inducible nitric oxide synthase (iNOS) expression in rats with monocrotaline (MCT)-induced pulmonary hypertension (data presented as mean  $\pm$  SD, n=7)

Statistical comparisons were conducted using a two-way analysis of variance (ANOVA) followed by Tukey's post hoc test.

The significance levels are represented as \* $P$ <0.05, \*\* $P$ <0.01, and \*\*\* $P$ <0.001.

$16.60 \pm 2.95 \text{ ng/ml}$  ( $P$ <0.001). Alamandine treatment reduced iNOS levels to  $182.10 \pm 45.65 \text{ ng/ml}$  in the MCT+Ala group ( $P$ <0.001) (Figure 3).

#### Effect of co-administration of MCT and alamandine on inflammatory cytokines

MCT significantly increased TNF- $\alpha$  levels ( $234.50 \pm 51.91 \text{ pg/ml}$ ) compared to the control group ( $41.29 \pm 6.47 \text{ pg/ml}$ ,  $P$ <0.001). Co-administration with alamandine lowered TNF- $\alpha$  levels to  $109.50 \pm 18.12 \text{ pg/ml}$  in the MCT+Ala group ( $P$ <0.001).

MCT administration raised NF- $\kappa$ B levels ( $16.82 \pm 4.92 \text{ pg/ml}$ ) compared to the control group ( $2.88 \pm 1.79 \text{ pg/ml}$ ,  $P$ <0.001). Co-administration with alamandine mitigated this increase to  $0.96 \pm 0.23 \text{ pg/ml}$  in the MCT+Ala group ( $P$ <0.01).

For IL-6, MCT significantly increased levels ( $71.36 \pm 4.73 \text{ pg/ml}$ ,  $P$ <0.001), which were moderated by alamandine to  $26.88 \pm 9.60 \text{ pg/ml}$  in the MCT+Ala group ( $P$ <0.001).

IL-1 $\beta$  levels surged with MCT administration ( $229.60 \pm 15.25 \text{ pg/ml}$ ,  $P$ <0.001) and were reduced to  $105.30 \pm 14.50$  in the MCT+Ala group ( $P$ <0.001) (Figure 4).

#### Histopathological findings

Figure 5 shows a cross-section of rat lung tissue stained with hematoxylin and eosin. Based on the obtained results, it was found that the amount of inflammation, secretion of mucus, bleeding inside the lung tissue, and secretion from inflammatory cells in the MCT group were higher than in other groups. In addition, the results showed that the amounts of these evaluated factors were high in the (MCT + Ala) group but lower than in the MCT group. Examining the images obtained from the control group showed ciliated cells with a normal appearance in bronchiole tissues. Air sacs with a pneumocyte cell layer were observed. In this row of cells, type 1 alveolar cells, which are very thin squamous cells, covered 95% of the alveolar surface and created a

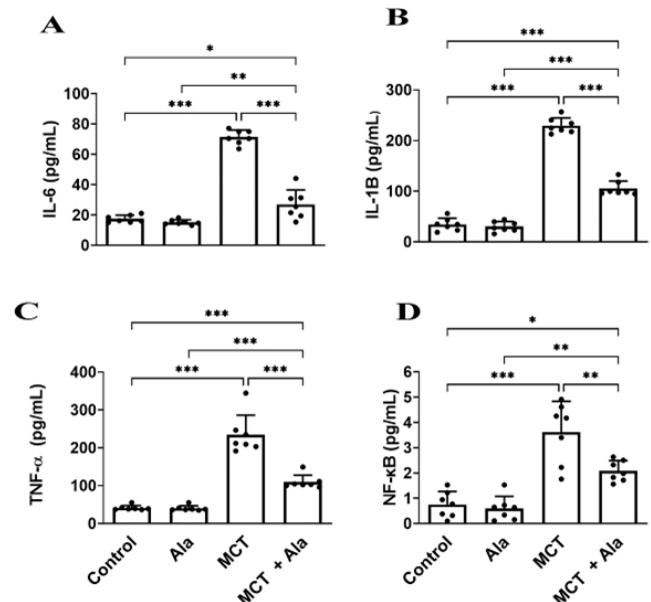


**Figure 4.** Inflammatory cytokines in rats with monocrotaline (MCT)-induced pulmonary hypertension

(A) Interleukin 6 levels in lung tissue, (B) Interleukin-1 beta (IL-1 $\beta$ ) levels in lung tissue, (C) Tumour necrosis factor-alpha (TNF- $\alpha$ ) levels in lung tissue, and (D) Nuclear factor kappa B (NF- $\kappa$ B) cell content in lung tissue (data presented as mean  $\pm$  SD, n=7). Statistical comparisons were performed using two-way analysis of variance (ANOVA) followed by Tukey's post hoc test.

Significance levels were denoted as \*\* $P$ <0.01, \*\*\* $P$ <0.001, and \* $P$ <0.05.

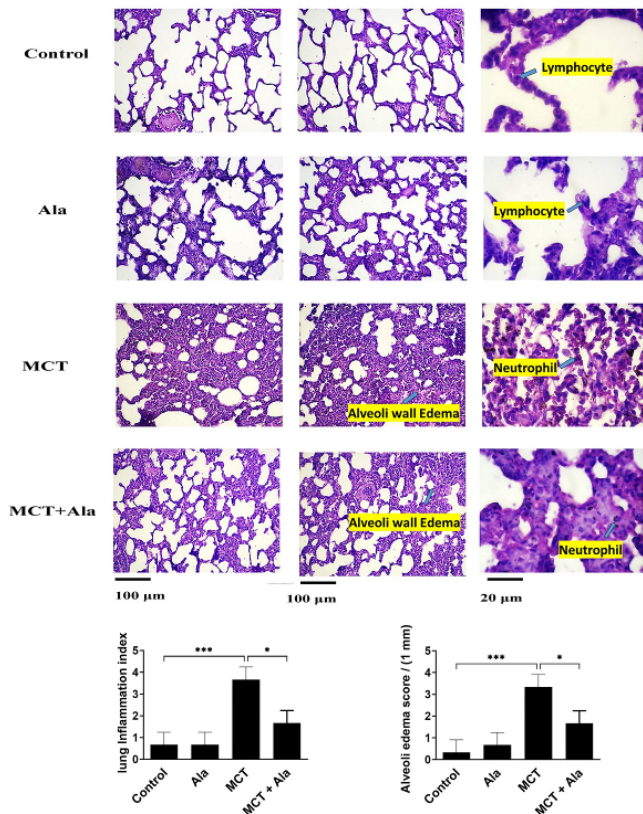


**Figure 5.** Histological sections of lung tissue from rats in the following groups: control group, monocrotaline (MCT)-treated group, alamandine group, and MCT + alamandine group. Hematoxylin and eosin staining at  $\times 100$  magnification (data presented as mean  $\pm$  SD). The significance levels were denoted as  $**P < 0.01$ ,  $***P < 0.001$ , and  $P < 0.05$ .

barrier between the air and the alveolar wall. Also, type 2 alveolar cells, which are cells that secrete surfactant, were observed normally in this group. In general, the tissue was completely normal without any thickening or signs of cellular metaplasia. The images related to the group (MCT + Ala) showed that the bronchioles in this group had a normal appearance. Among the cells, bleeding effects were greatly reduced compared to the MCT group (Figure 5).

#### Immunofluorescence for MrgD Receptors in lungs

The immunofluorescence staining of MrgD receptors was significantly increased in the lung tissue of MCT-treated rats compared to those from control rats ( $P < 0.001$ ). Alamandine treatment significantly decreased MrgD receptor levels compared with the MCT group ( $P < 0.01$ ) (Figure 6).

#### Discussion

In the present study, we showed that administration of alamandine had protective effects on MCT-induced PAH in rats. These effects could be linked to the reduction in oxidative stress and inflammatory cytokine levels. These positive effects have been discussed previously (31, 32) defined as a mean pulmonary artery pressure by right-sided heart catheterization of at least 25 mm Hg at rest. It is classified into 5 general groups based on the underlying cause, with left ventricular failure and chronic obstructive pulmonary disease being 2 of the most common causes in the United States. Although the specifics of the pathophysiology will vary with the cause, appreciating the risks of pulmonary hypertension and right ventricular failure is critical to

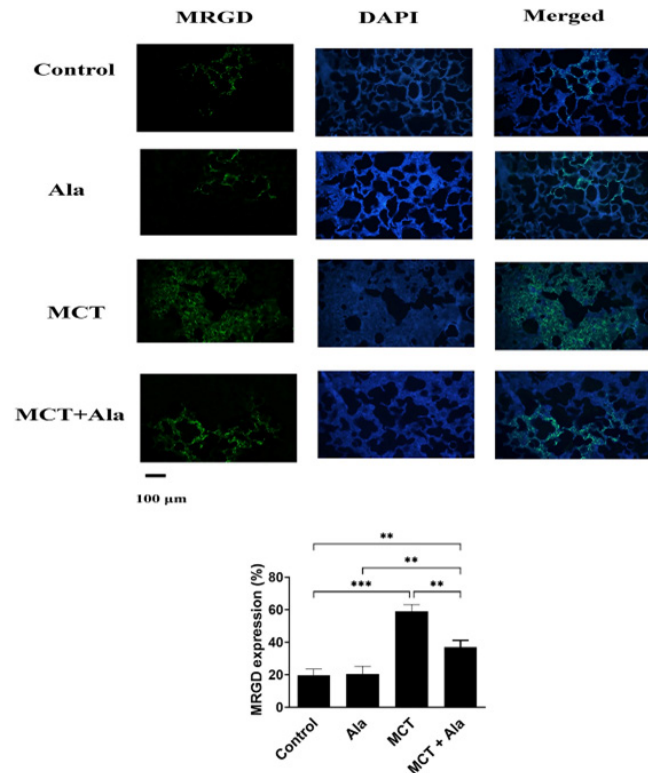


**Figure 6.** Immunofluorescence detection of Mas-related G protein-coupled receptor member D (MrgD) in the lungs of rats

Triple immunostaining was performed to visualize the MrgD receptor (green) and nucleus with DAPI (blue). Representative images showed the expression of MrgD in the lung membrane. Quantitative analysis revealed a higher expression of MrgD in the monocrotaline (MCT)-induced pulmonary hypertension group compared to the control group. However, a decreased expression of MrgD was observed in the MCT + alamandine group compared to the MCT group. The significance levels were denoted as  $**P < 0.01$ ,  $***P < 0.001$ , and  $P < 0.05$ .

appropriately evaluating and resuscitating pulmonary hypertension patients in the emergency department (ED). PAH is characterized by undesirable hemodynamic changes in pulmonary arteries. These changes give rise to a significant increase in PAH and RVSP along with RVH. In animal models, similar changes, RVSP and RVH are commonly considered evidence of the presence of PAH (33, 34).

The major findings of this investigation are that alamandine suppressed inflammation, reduced reactive oxygen species, and restored injuries to lung tissue caused by oxidative stress. This study showed that alamandine ameliorated PAH, as demonstrated by the improved right ventricular systolic pressure and resolved RV/(LV+SP) weight ratio. Compared with the MCT group, the rats that received alamandine therapies showed improvements in the right hemodynamic parameters (i.e., RVSP). It has been shown that alamandine induces vasodilatory and anti-hypertensive effects through the MrgD receptor (35) and that the reduction of RVSP is probably due to a decline in afterload produced by alamandine action (34). MCT exerted a significant decrease in final body weight, which is a sign of heart failure. This phenomenon is similar to cachexia in chronic heart failure patients. The growth restriction has been reported to be induced by MCT administration; in a previous study, rats became severely anorexic upon exposure to MCT (36). Body weight loss has also been shown to accompany a significant increase in RV/body weight and RV/LV+S ratios, indicating RVH. The observed increase in the lung-to-body weight ratio within the MCT

group can potentially serve as an indicator of extensive pulmonary proliferative response (37). However, due to the concurrent reduction in body weight attributed to the effects of monocrotaline, this parameter may not serve as a precise indicator.

In the MCT-treated group, significant reductions in heart rate, QRS amplitude, and duration were observed. The decreases in HR and QRS amplitude could be a result of down-regulation of the  $\beta_1$ -adrenoceptor and desensitization of the  $\beta_1$ -adrenoceptor-G protein-adenylyl cyclase system due to MCT's effect, followed by RVH (38). Moreover, MCT's direct cardiotoxic action and coronary artery medial wall-thickening effect could influence the depression of ventricular function (22). Also, RVH may contribute to the impairment of electromotive forces via a reduction in mean QRS vector magnitude (39). When treatment was combined with alamandine, RV/body weight and lung/body weight ratios normalized, and the RV/LVS ratio significantly decreased compared to the MCT group. QRS amplitude was also normalized.

Three main factors are known as contributors to the development and progression of endothelial injury in PAH, namely, inflammation, NO, and oxidative stress. Inflammation is considered to be a major factor in initiating and maintaining vascular remodeling in PAH animal models (40). Consequently, reducing the inflammatory response might ameliorate PAH development. Previous studies have indicated that the TNF- $\alpha$  level in heritable and idiopathic PAH patients was considerably higher than in healthy individuals (41, 42). Our data demonstrated statistically significant reductions in TNF- $\alpha$ , IL-1 $\beta$ , and IL-6 levels ( $P < 0.001$ ), as well as NF- $\kappa$ B levels ( $P < 0.05$ ), in the alamandine-treated group compared to the MCT-induced PAH group. These findings indicate that alamandine counteracts the inflammatory response in MCT-induced PAH rats.

NO, produced by the nitric oxide synthases (NOSs) family, is an often-recognized key factor contributing to the development and progression of endothelial injury in PAH. Within this family, iNOS stands out as an inducible member that generates a sustained production of NO after induction (43). The course of PAH induced by MCT injection is progressive, with persistent inflammation defined by an acute phase within the first 6 days after MCT treatment, followed by a chronic phase (44). There is no or little expression of iNOS in normal tissue; obvious iNOS expression can occur only in cases of acute or chronic inflammation (45). MCT treatment overactivated the NO signaling pathway. The activation of iNOS generated a large amount of NO, which, in turn, contributed to a further deterioration of the vascular endothelial cells (46). In this study, MCT significantly increased iNOS, while co-administration of alamandine and MCT decreased NOS. This reduction could be a result of a decrease in the inflammatory factors associated with alamandine.

A study demonstrated that both SOD and glutathione peroxidase activities decreased in PAH lungs when compared to healthy controls (47). Furthermore, Irodova *et al.* showed an increase in the level of MDA in PAH patients in comparison to healthy controls (48). This elevation was more prominent in patients with severe pulmonary hypertension, while the results of glutathione peroxidase activity were inconclusive. In this study, we discussed three well-studied oxidative stress biomarkers in tissues (i.e., CAT and SOD enzyme activity), as well as MDA levels. The first two biomarkers represent the core of the

enzymatic antioxidant system. Generally, SODs catalyze the conversion of superoxide radicals to  $H_2O_2$ , which, in turn, is converted into water by CAT. As shown *in vivo*, SOD and CAT mimetics can reverse pulmonary vascular remodeling and PAH. Therefore, it is likely that these enzymes' activities have pathologic values in PAH patients (48). MDA can be a marker for lipid peroxidation and can be used to indirectly assess the intensity of damage to cell membranes (49). In our study, the MDA levels were significantly decreased as a result of co-administration of alamandine and MCT. On the other hand, levels of SOD and CAT enzyme activity increased. The results of our experiment are consistent with those of a previous study in which alamandine increased antioxidant protein expression in ventricles exposed to I/R injuries (50). Moreover, inhibiting the PKC/reactive oxygen species signaling pathway reduced renal damage in Dahl rats (51).

In this study, we also investigated the expression of MrgD receptors. Alamandine performs its actions by binding to the MrgD receptor (16, 25, 35, 52). We found that MrgD expression was higher in the lungs of the MCT group than in the group that received the co-administration of alamandine and MCT, suggesting that alamandine receptor activity is enhanced in the lungs during pulmonary hypertension. Previously reported studies have indeed shown an up-regulation of MrgD expression in various hypertensive conditions (53). For instance, the MrgD expression is increased in the heart of spontaneously hypertensive rats (54) and ventricular myocytes from the TGR (mREN2)27 rat model of hypertension (55). This up-regulation under pathological scenarios underscores the potential protective role MrgD might play during the course of disease progression (53). Importantly, our study further explores this avenue by demonstrating that alamandine treatment leads to a reduction in MrgD receptor levels, which is concomitant with decreased pulmonary arterial pressure. This implies a mechanistic link between MrgD receptor modulation and PAH. The relationship between alamandine, MrgD receptors, and pulmonary arterial pressure offers a promising avenue for therapeutic interventions and warrants further investigation.

These results provide evidence that alamandine may be a protective agent in the treatment of pulmonary hypertension.

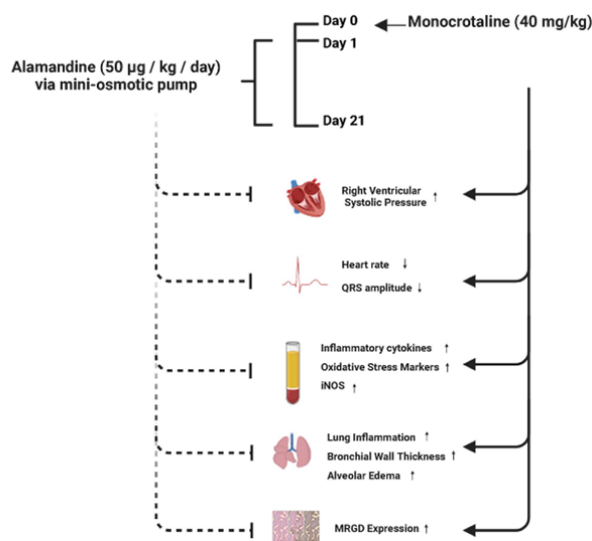


**Figure 7.** Comprehensive overview of alamandine's impact on pulmonary hypertension: Attenuation of doxorubicin-induced cardiac contractility reduction, ECG abnormalities, elevated inflammatory cytokines, and lung inflammation

Furthermore, our findings are effectively summarized in the graphical abstract (Figure 7), which provides a visual representation of the key results and insights presented in this study.

### Conclusion

Our study demonstrated that alamandine effectively mitigated MCT-induced PAH in rats. It achieved this by reducing oxidative stress, inflammation, regulating inducible nitric oxide synthase, and ameliorating histopathological changes. The observed elevation in MrgD expression in the context of PAH may have signified a compensatory mechanism initiated to counteract the effects of PAH and potentially restore pulmonary homeostasis. Notably, alamandine treatment, by reducing PAH, may have counteracted this increase in MrgD expression, highlighting its role in regulating this compensatory response. These findings underscored the therapeutic promise of alamandine in managing PAH.

### Acknowledgment

The results presented in this paper were part of Freshteh Amini's thesis. This study was funded by Fasa University of Medical Sciences, Iran (grant number 400303).

### Authors' Contributions

A SH and K J conceived the study and designed the experiments. F A and A SH were responsible for conducting the research. A SH and K J performed data analysis and also wrote the manuscript. All authors have thoroughly reviewed and approved the final version of the manuscript.

### Funding

This study was funded by Fasa University of Medical Sciences, Iran (grant number 400303).

### Ethics Committee Approval

Animals were approved by Fasa University of Medical Sciences with the ethical code (IR.FUMS.AEC.1401.010), obtained on September 7, 2022.

### Conflicts of Interest

The authors declare that they have no conflicts of interest concerning the research, authorship, and/or publication of this article.

### References

1. Maron BA. Revised definition of pulmonary hypertension and approach to management: A clinical primer. *J Am Heart Assoc* 2023; 12: e029024.
2. Rajagopal S, Ruetzler K, Ghadimi K, Horn EM, Kelava M, Kudelko KT, *et al.* Evaluation and management of pulmonary hypertension in noncardiac surgery: A scientific statement from the American Heart Association. *Circulation* 2023; 47: 1317–1343.
3. Benza RL, Miller DP, Barst RJ, Badesch DB, Frost AE, and McGoon MD. An evaluation of long-term survival from time of diagnosis in pulmonary arterial hypertension from the reveal registry. *Chest* 2012; 142: 448–456.
4. Tobal R, Potjewijd J, van Empel VPM, Ysermans R, Schurgers LJ, Reutelingsperger CP, *et al.* Vascular remodeling in pulmonary arterial hypertension: The potential involvement of innate and adaptive immunity. *Front Med* 2021; 8: 806899.
5. Stenmark KR, Meyrick B, Galie N, Mooi WJ, McMurtry IF. Animal models of pulmonary arterial hypertension: the hope for etiological discovery and pharmacological cure. *Am J Physiol Lung Cell Mol Physiol* 2009; 297: 1013–32.
6. Yan Q, Liu S, Sun Y, Chen C, Yang S, Lin M, *et al.* Targeting oxidative stress as a preventive and therapeutic approach for cardiovascular disease. *J Transl Med* 2023; 21: 519.
7. Bekedam FT, Goumans MJ, Bogaard HJ, de Man FS, and Lluçà-Valldeperas A. Molecular mechanisms and targets of right ventricular fibrosis in pulmonary hypertension. *Pharmacol Ther* 2023; 244: 108389.
8. Guignabert C, Tu L, Girerd B, Ricard N, Huertas A, Montani D, *et al.* New molecular targets of pulmonary vascular remodeling in pulmonary arterial hypertension: Importance of endothelial communication. *Chest* 2015; 147: 529–537.
9. Balabanian K, Foussat A, Dorfmueller P, Durand-Gasselini I, Capel F, Bouchet-Delbos L, *et al.* CX(3)C chemokine fractalkine in pulmonary arterial hypertension. *Am J Respir Crit Care Med* 2002; 165: 1419–1425.
10. Kommireddy S, Bhyravajhala S, Kurimeti K, Chennareddy S, Kanchinadham S, Vara Prasad IR, *et al.* Pulmonary arterial hypertension in systemic lupus erythematosus may benefit by addition of immunosuppression to vasodilator therapy: An observational study. *Rheumatology (Oxford)* 2015; 54: 1673–1679.
11. Campos M and Schioppa E. Pulmonary arterial hypertension in adult-onset Still's disease: Rapid response to anakinra. *Case Rep Rheumatol* 2012; 2012: 1–5.
12. Sakuma M, Toyoda S, Inoue T, and Node K. Inflammation in pulmonary artery hypertension. *Vascul Pharmacol* 2019; 118–119: 106562.
13. Wu XH, Ma JL, Ding D, Ma YJ, Wei YP, and Jing ZC. Experimental animal models of pulmonary hypertension: Development and challenges. *Anim Model Exp Med* 2022; 5: 207–216.
14. Sato T, Suzuki T, Watanabe H, Kadowaki A, Fukamizu A, Liu PP, *et al.* Apelin is a positive regulator of ACE2 in failing hearts. *J Clin Invest* 2013; 123: 5203–5211.
15. Marshall RP. The pulmonary renin-angiotensin system. *Curr Pharm Des* 2003; 9: 715–722.
16. Soltani Hekmat A, Javanmardi K, Kouhpayeh A, Baharamali E, Farjam. Differences in cardiovascular responses to alamandine in two-kidney, one clip hypertensive and normotensive rats. *Circ J* 2017; 81: 405–412.
17. Soltani Hekmat A and Javanmardi K. Alamandine: Potential protective effects in SARS-CoV-2 patients. *J Renin Angiotensin Aldosterone Syst* 2021; 202: 6824259.
18. Soltani Hekmat A, Navabi Z, Alipanah H, and Javanmardi K. Alamandine significantly reduces doxorubicin-induced cardiotoxicity in rats. *Hum Exp Toxicol* 2021; 10: 1781–1795.
19. Park BM, Phuong HTA, Yu L, and Kim SH. Alamandine protects the heart against reperfusion injury via the MrgD receptor. *Circ J* 2018; 82: 2584–2593.
20. De Souza-Neto FP, De Moraes E Silva M, De Carvalho Santuchi M, De Alcântara-Leonídio TC, Motta-Santos D, Oliveira AC, *et al.* Alamandine attenuates arterial remodeling induced by transverse aortic constriction in mice. *Clin Sci* 2019; 133: 629–643.
21. Li P, Chen X-RR, Xu F, Liu C, Li C, Liu H, *et al.* Alamandine attenuates sepsis-associated cardiac dysfunction via inhibiting MAPKs signaling pathways. *Life Sci* 2018; 206: 106–116.
22. Hekens IR, Mouchaers KTB, Vliegen HW, van Der Laarse WJ, Swenne CA, Maan AC, *et al.* Early changes in rat hearts with developing pulmonary arterial hypertension can be detected with three-dimensional electrocardiography. *Am J Physiol Heart Circ Physiol* 2007; 293: 1300–1307.
23. Soltani Hekmat A, Chenari A, Alipanah H, and Javanmardi K. Protective effect of alamandine on doxorubicin-induced nephrotoxicity in rats. *BMC Pharmacol Toxicol* 2021; 22: 31.
24. Liu Q, Zheng B, Zhang Y, Huang W, Hong Q, and Meng Y.

- Alamandine via MrgD receptor attenuates pulmonary fibrosis via NOX4 and autophagy pathway. *Can J Physiol Pharmacol* 2021; 99: 885–93.
25. Soltani Hekmat A, Zare N, Moravej A, Meshkibaf MH, Javanmardi K. Effect of prolonged infusion of alamandine on cardiovascular parameters and cardiac ACE2 expression in a rat model of renovascular hypertension. *Biol Pharm Bull* 2019; 42: 960–967.
  26. Lan W, Chi L, Xiru C, and Peng L. Alamandine attenuates long-term hypertension-induced cardiac fibrosis independent of blood pressure. *Mol Med Rep* 2019; 19: 4553–4560.
  27. Sutendra G and Michelakis ED. Pulmonary arterial hypertension: challenges in translational research and a vision for change. *Sci Transl Med* 2013; 5: 208sr5.
  28. Dianat M, Radan M, Badavi M, Mard SA, Bayati V, and Ahmadzadeh M. Crocin attenuates cigarette smoke-induced lung injury and cardiac dysfunction by anti-oxidative effects: The role of Nrf2 antioxidant system in preventing oxidative stress. *Respir Res* 2018; 19: 58.
  29. Musa AE, Shabeeb D, and Alhilfi HSQ. Protective effect of melatonin against radiotherapy-induced small intestinal oxidative stress: Biochemical evaluation. *Medicina (Kaunas)* 2019; 55: 308.
  30. Hasan HF, Abdel-Hamid GR, and Ebrahim SI. Antioxidant and anti-inflammatory effects of diallyl disulfide on hepatotoxicity induced by cyclophosphamide in rats. *Nat Prod Commun* 2020; 15: 1-10.
  31. Wilcox SR, Kabrhel C, and Channick RN. Pulmonary hypertension and right ventricular failure in emergency medicine. *Ann Emerg Med* 2015; 66: 619–628.
  32. Cajigas HR and Awdish R. Classification and diagnosis of pulmonary hypertension. *Heart Fail Rev* 2016; 21: 229–237.
  33. Csiszar A, Labinsky N, Olson S, Pinto JT, Gupte S, Wu JM, et al. Resveratrol prevents monocrotaline-induced pulmonary hypertension in rats. *Hypertens* 2009; 54: 668–675.
  34. Fan YF, Zhang R, Jiang X, Wen L, Wu DC, Liu D, et al. The phosphodiesterase-5 inhibitor vardenafil reduces oxidative stress while reversing pulmonary arterial hypertension. *Cardiovasc Res* 2013; 99: 395–403.
  35. Lautner RQ, Villela DC, Fraga-Silva RA, Silva N, Verano-Braga T, Costa-Fraga F, et al. Discovery and characterization of alamandine. *Circ Res* 2013; 112: 1104–1111.
  36. Koo HS, Kim KC, and Hong YM. Gene expressions of nitric oxide synthase and matrix metalloproteinase-2 in monocrotaline-induced pulmonary hypertension in rats after bosentan treatment. *Korean Circ J* 2011; 41: 83–90.
  37. Leineweber K, Seyfarth T, Abraham G, Gerbershagen HP, Heinroth-Hoffmann I, Pönicke K, et al. Cardiac beta-adrenoceptor changes in monocrotaline-treated rats: Differences between membrane preparations from whole ventricles and isolated ventricular cardiomyocytes. *J Cardiovasc Pharmacol* 2003; 41: 333–342.
  38. Akhavein F, Jean St-Michel E, Seifert E, and Rohlicek C V. Decreased left ventricular function, myocarditis, and coronary arteriolar medial thickening following monocrotaline administration in adult rats. *J Appl Physiol* 2007; 103: 287–295.
  39. Sharma RK, Oliveira AC, Kim S, Rigatto K, Zubecevic J, Rathinasabapathy A, et al. Involvement of neuroinflammation in the pathogenesis of monocrotaline-induced pulmonary hypertension. *Hypertension* 2018; 71: 1156–1163.
  40. Hemnes AR, Rathinasabapathy A, Austin EA, Brittain EL, Carrier EJ, Chen X, et al. A potential therapeutic role for angiotensin-converting enzyme 2 in human pulmonary arterial hypertension. *Eur Respir J* 2018; 51: 1702638.
  41. Cohen-Kaminsky S, Hautefort A, Price L, Humbert M, and Perros F. Inflammation in pulmonary hypertension: what we know and what we could logically and safely target first. *Drug Discov Today* 2014; 19: 1251–1256.
  42. Soon E, Holmes AM, Treacy CM, Doughty NJ, Southgate L, MacHado RD, et al. Elevated levels of inflammatory cytokines predict survival in idiopathic and familial pulmonary arterial hypertension. *Circulation* 2010; 122: 920–927.
  43. Kurakula K, Smolders VFED, Tura-Ceide O, Wouter Jukema J, Quax PHA, and Goumans MJ. Endothelial dysfunction in pulmonary hypertension: Cause or consequence? *Biomedicines* 2021; 9: 1–23.
  44. Tang C, Luo Y, Li S, Huang B, Xu S, and Li L. Characteristics of inflammation process in monocrotaline-induced pulmonary arterial hypertension in rats. *Biomed Pharmacother* 2021; 133: 111081.
  45. Long M, Yang SH, Han JX, Li P, Zhang Y, Dong S, et al. The protective effect of grape-seed proanthocyanidin extract on oxidative damage induced by zearalenone in kunming mice liver. *Int J Mol Sci* 2016; 17: 808.
  46. Wang X, Yang Y, Yang D, Tong G, Lv S, Lin X, et al. Tetrandrine prevents monocrotaline-induced pulmonary arterial hypertension in rats through regulation of the protein expression of inducible nitric oxide synthase and cyclic guanosine monophosphate-dependent protein kinase type 1. *J Vasc Surg* 2016; 64: 1468–1477.
  47. Cracowski JL, Cracowski C, Bessard G, Pepin JL, Bessard J, Schwebel C, et al. Increased lipid peroxidation in patients with pulmonary hypertension. *Am J Respir Crit Care Med* 2001; 164: 1038–1042.
  48. Irodova NL, Lankin VZ, Konovalova GK, Kochetov AG, and Chazova IE. Oxidative stress in patients with primary pulmonary hypertension. *Bull Exp Biol Med* 2002; 133: 580–582.
  49. DeMarco VG, Habibi J, Whaley-Connell AT, Schneider RI, Heller RL, Bosanquet JP, et al. Oxidative stress contributes to pulmonary hypertension in the transgenic (mRen2)27 rat. *Am J Physiol Heart Circ Physiol* 2008; 294: H2659–68.
  50. Tacar O, Sriamornsak P, and Dass CR. Doxorubicin: An update on anticancer molecular action, toxicity and novel drug delivery systems. *J Pharm Pharmacol*. 2013; 65: 157–170.
  51. Dobashi K, Ghosh B, Orak JK, Singh I, and Singh AK. Kidney ischemia-reperfusion: Modulation of antioxidant defenses. *Mol Cell Biochem* 2000; 205: 1-11.
  52. Gong J, Luo M, Yong Y, Zhong S, and Li P. Alamandine alleviates hypertension and renal damage via oxidative-stress attenuation in Dahl rats. *Cell Death Discov* 2022; 8: 1–9.
  53. Jesus ICG, Mesquita T, Souza Santos RA, and Guatimosim S. An overview of alamandine/MrgD signaling and its role in cardiomyocytes. *Am J Physiol Cell Physiol* 2023; 324: 606–613.
  54. Liu C, Yang C-X, Chen X-R, Liu B-X, Li Y, Wang X-Z, et al. Alamandine attenuates hypertension and cardiac hypertrophy in hypertensive rats. *Amino Acids* 2018; 50: 1071–1081.
  55. Jesus ICG, Mesquita TRR, Monteiro ALL, Parreira AB, Santos AK, Coelho ELX, et al. Alamandine enhances cardiomyocyte contractility in hypertensive rats through a nitric oxide-dependent activation of CaMKII. *Am J Physiol Cell Physiol* 2020; 318: 740–750.